

Lasers in Manufacturing Conference 2021

Influence of defocusing in deep penetration welding of copper by using visible wavelength

Florian Kaufmann^{a,*}, Andreas Meier^a, Jakob Ermer^{a,b}, Stephan Roth^{a,b} and Michael Schmidt^{a,b,c}

^aBayerisches Laserzentrum GmbH, Konrad-Zuse-Straße 2/6, 91052 Erlangen, Germany

^bErlangen Graduate School in Advanced Optical Technologies (SAOT), Paul-Gordan-Straße 6, 91052 Erlangen, Germany

^cInstitute of Photonic Technologies, Friedrich-Alexander-Universität Erlangen-Nürnberg, Konrad-Zuse-Straße 3/5, 91052 Erlangen, Germany

Abstract

High-quality joining of copper materials has become a key factor in many electric applications like electric engines, batteries or power electronics. By now high-power laser beam sources emitting visible laser radiation are available to promote the already well-suited joining method of laser beam welding. Consequently, this process can now face the challenges of welding highly reflective materials, such as copper, which originate mainly in the low absorptivity of conventionally used infrared wavelengths at room temperature and the rapid jump of the absorption at the transition from solid to liquid state. However, up to now mostly the heat conduction welding process has been examined and the effects of shorter wavelengths on deep penetration welding have been neglected. Thus, for this work the scope lies on the wavelength dependent intensity needed to overcome the deep penetration welding threshold and the alteration of energy incoupling into the vapour capillary using green wavelength and defocusing.

Keywords: visible wavelength, green laser beam, copper, deep penetration welding, energy incoupling

* Corresponding author. Tel.: +49-913-197-7900; fax: +49-913-197-79011.
E-mail address: info@blz.org.

1. Introduction and state of the art

Due to increasing importance of e-mobility, copper is a material that is widely used in drive and battery technology these days. Due to its high electrical and thermal conductivity, it is predestined for applications for conducting electricity as well as for heat dissipation. Laser beam welding is a joining technique that has become an indispensable part of body in white production in automotive industry. Until now, this process is mainly dominated by laser beam sources of infrared wavelengths. When contacting electrical components, one inevitably encounters laser beam welding of copper as a favorable joining technology. For this combination, high quality results can be achieved in deep welding mode within a limited process window [1]. Since the ratio of weld seam depth to width (aspect ratio) is comparably large here, it is more likely to be used for thick components like in hairpin welding [2]. Outside the process window (resulting from laser power and feed rate), which is comparably small with regard to steel, the process has a strong tendency to spatter ejection and inhomogeneous welding seam depth [3]. A reason for that behavior is seen in the low absorptivity of the infrared laser radiation in copper and in a sudden increase in absorptivity during the phase transition from solid to liquid respectively [4]. The latter effect is reinforced by multiple reflection of the laser beam, which occurs as soon as a vapor capillary is formed and the process thus changes from heat conduction to deep penetration welding mode. To overcome the drawbacks of a limited process window, processing of copper with visible laser wavelength can be an attractive solution to exploit the benefits of higher absorptivity of electromagnetic waves in metals [5]. This is expected to allow better control of the welding process which plays an important role for example for safety reasons when contacting battery cells. This approach is already investigated for different green laser beam sources for various welding regimes [6] and process guidance strategies [7]. All these approaches show application benefits, allowing promising broader flexibility in copper joining. Results show a significant process stabilization in heat conduction welding [8]. Nevertheless, process restrictions remain, since spattering especially at low feed rates is observed and blowing the vapor plume out of the beam path is required [6]. Therefore, fundamental analysis of dominating process mechanisms in copper welding with different laser wavelengths with regard to process results is necessary to differentiate the capabilities of this joining technology for industrial environment. For this purpose, laser beam welding of copper with infrared and green laser beam sources is investigated from different perspectives within this work. It is expected, that working with larger spot diameters by means of defocusing still shows stable deep penetration welding results when using green laser radiation because of higher absorptivity. An influence on the resulting properties of the weld seam as well as melt ejections is suspected and hence investigated.

2. Aims and Methods

For comparison of visible and infrared laser radiation two disk lasers from TRUMPF Laser- und Systemtechnik GmbH, Germany were used which generate laser beams of similar optical properties. For specifications see Table 1.

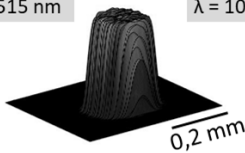
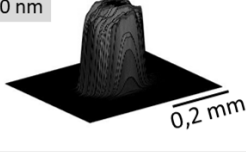
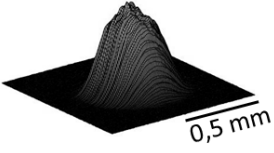
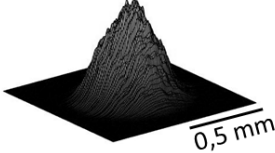
Table 1: Properties of laser beam sources investigated within this work

Description	TruDisk 3022	TruDisk 8001
Wavelength λ	515 nm (green)	1030 nm (infrared)
Maximum laser power P_{Max}	3000 W	8000 W
Fibre core diameter	200 μm	200 μm
Rayleigh length z_R	1.22 mm	1.61 mm

In each setup an optical fibre with a core diameter of 200 μm guides the laser beam to a fixed optics system (TRUMPF BEOD70). Since both optics possess equal image ratio of 1.0 a comparison of the performance of the two laser beams is possible. The presented experiments were conducted with different spot diameters between 200 μm and 750 μm . The latter one is accomplished by defocusing the laser beam of 3.5 Rayleigh lengths. The resulting spot diameters and beam intensity profiles can be seen in Table 2 respectively. The measurements were carried out with a Focus Monitor FM from PRIMES GmbH, Germany. Other than that, the system architecture remains unaltered.

As can be seen, the laser beams have a clear top hat intensity profile in the focal plane. Gaussian intensity profile with a relatively sharp top is observed in the case of defocusing. This is done in direction where the point of highest intensity is outside the workpiece. The diameter of this mode expands with increasing defocus-

Table 2: Beam intensity profiles of both laser beams using a 200 μm optical fibre and laser welding optics (Trumpf BEOD 70)

Spot diameter d_F in focal plane	200 μm
Beam intensity profile in focal plane	<div> <div>$\lambda = 515 \text{ nm}$</div>  </div>
	<div> <div>$\lambda = 1030 \text{ nm}$</div>  </div>
Spot diameter d_F at defocusing of $2 z_R$	480 μm
Beam intensity profile at defocusing of $2 z_R$	
	

sing. Bead on plate welds were conducted using 3 mm thick Cu-ETP samples since this material is often needed for current-carrying applications in automotive industry [9]. Apart from Cu, which has to be at least 99,9 %, a maximum oxygen content of 0,04 % is tolerated within this material.

Laser beam welding experiments have been carried out according to parameter settings depicted in Table 3. Therefore, application relevant feed rates from 2 m/min to 20 m/min and laser powers up to the operating maximum of the laser systems were chosen.

Table 3: Parameters of the experimental study in this work

Dimension	Unit	Choice of parameters
Material of sample	[-]	Cu-ETP
Feed rate v	[m/min]	2 - 20
Power of laser P	[kW]	1 - 3 @ green 1 - 8 @ IR
Welding mode	[-]	continuous wave
Beam diameter	[μm]	200 - 750

The experimental setup for $\lambda = 515 \text{ nm}$ is shown in Figure 1. The welding optics is attached to a Kuka KRC 90 6-axis robot, allowing flexible positioning of the focal plane. The samples were fixed in a clamping device,

arranged on a horizontal linear axis, ensuring a stationary process zone. The optics were tilted 10° in weld direction in order to prevent damages by back reflecting laser light. Consequently, An incident angle of the laser beam of 10° to the surface normal of the copper sample prevails. As angular dependence of the absorptivity of copper at 515 nm and 1030 nm does not show significant differences in this angular range (see Ref. [10]), the influence in regard to horizontal incident beam can be neglected for discussed process results in this paper. To avoid influence of oxide layer, the samples were sandblasted and cleaned with acetone prior welding. An ensemble of process nozzle and the suction unit ensured a constant flow over the workpiece

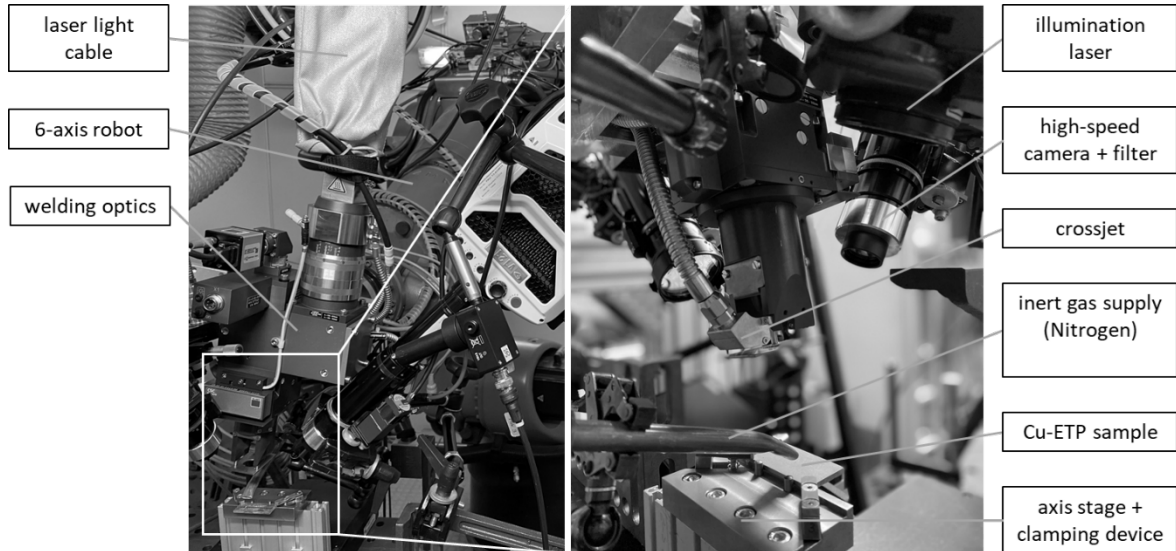


Fig. 1: Experimental setup for laser beam welding with $\lambda = 515$ nm

surface. The process nozzle was aligned to the process zone and covered the interaction zone continuously as the sample was moved forward. Weld seam lengths of $l = 45$ mm were generated, whereby Nitrogen was used as inert shielding gas. The influence of defocusing and altering the intensity profile on process instabilities, weld seam geometry and overcoming the deep welding threshold is investigated. Therefore, the samples were sectioned by abrasive cutting, embedded in epoxy resin, grinded, polished with $1\ \mu\text{m}$ diamond suspension and further polished with an active oxide polishing suspension (colloidal silica and hydrogenperoxide). Weld seam properties were measured by microscopic analysis after etching the samples with iron(III)-chloride.

Process observation have been conducted using high-speed imaging. Two high-speed cameras (VisionResearch Phantom v1210) working with a frame rate of 50 kHz using an image size of 512×320 pixel were mounted under an angle of 30 degrees to the workpiece normal, 45 degrees respectively. To evaluate capillary instabilities and spatter ejection from the irradiated zone and the melt pool, a side view on the interaction zone was chosen. For in detail analysis of the keyhole opening, the second camera was aligned to view the keyhole front wall against weld direction. To illuminate the keyhole region a laser system (Cavitar Cavilux HF, 808 nm, 500 W peak power) was used. Band-pass filters inserted in front of the camera objectives ensure that only the wavelength of the illumination laser reaches the imaging chip. Other disturbing light (e.g. brightness of the plasma plume and reflections of the processing laser) were blocked or reduced thereby. The high-speed recordings were analyzed using calibration videos to measure keyhole features and process instabilities (spatter, melt ejection) in comparison to used parameter settings quantitatively, see Table 3.

3. Results and Discussion

3.1. Influence of shielding gas on vapor plume interaction

Figure 2 (a) and (b) depict top sections and analysis of weld seam depth of Cu-ETP samples generated at different laser wavelengths of $\lambda = 515 \text{ nm}$ and $\lambda = 1030 \text{ nm}$. The diagram additionally depicts the influence of shielding gas on weld seam properties. In general it can be said that the absence of shielding gas leads to no significant difference in weld seam depth for infrared wavelength, whereas a 70 % higher weld depth is found in the case of Nitrogen application for $\lambda = 515 \text{ nm}$. Consequently, a significant part of laser energy is absorbed by the vapor plume in case it is not blown out of the beam path. Figure 3 shows representative high-speed images for both wavelength without usage of shielding gas. For this investigation laser illumination was switched off and optical filters were adopted to blocking range of laser wavelength in order to see a broader wavelength spectrum. A clear bright zone can be observed covering the area above the keyhole in case of green

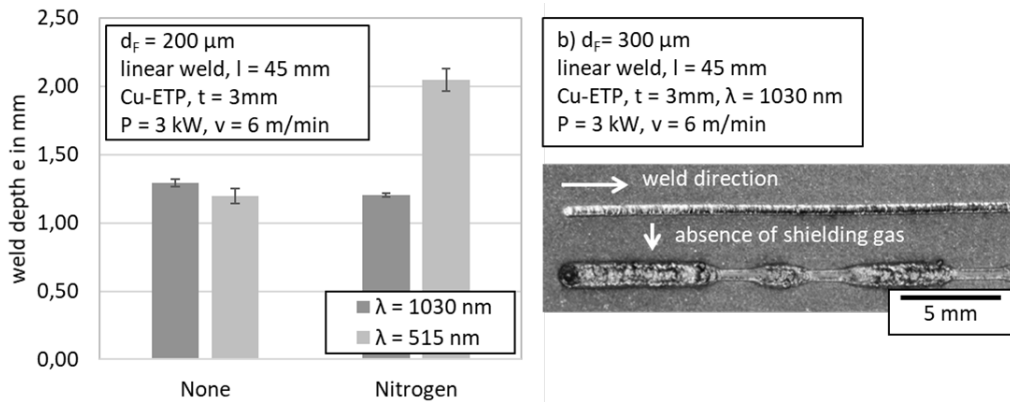


Fig. 2: Weld seam depth versus application of shielding gas for different laser wavelengths of $\lambda = 515 \text{ nm}$ and $\lambda = 1030 \text{ nm}$; (b) top sections of welded samples with and without shielding gas

laser wavelength. In contrast IR laser welding shows less interaction, identified by evidence of evaporating material emanating from the keyhole. The absorption of laser radiation in the vapor plume was also investigated by Zhang et al. [11] finding that the vapor plume interacts in different manner with incident laser beam. Depending on the metal and wavelength used, different shapes of emission spectra and properties were found. These observations are confirmed and detailed by presented investigations within this work.

Higher standard deviation in weld depth in case of $\lambda = 515 \text{ nm}$ using nitrogen shielding can be explained by higher absorptivity of green laser wavelength for copper material, see [12]. As a higher amount of copper gets

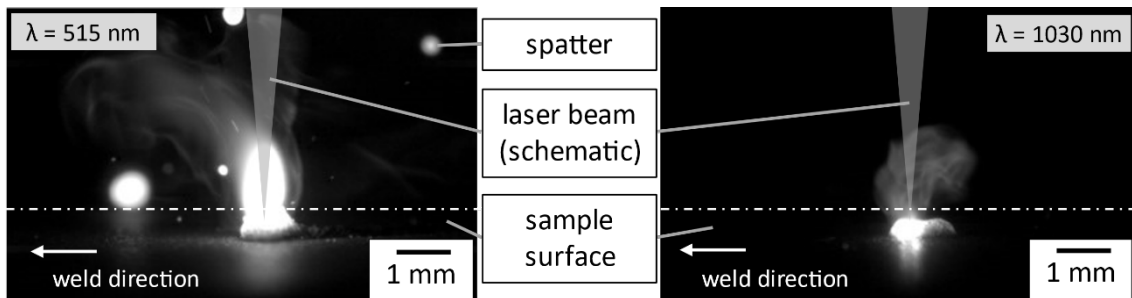


Fig. 3: Characteristic high-speed images of vapor plume interaction for different laser wavelengths, operating parameters: Cu-ETP, $t = 3 \text{ mm}$, $d_f = 200 \mu\text{m}$, $P = 3 \text{ kW}$, $v = 6 \text{ m/min}$, no shielding gas used

molten for equal laser power, increased molten volume promotes spattering at low feed rates. This leads to a greater fluctuation in the shape of weld seam cross-section. The behaviour is investigated further below.

Lower energy densities at $\lambda = 1030$ nm enable different coupling of the laser beam into the workpiece which is especially important if parameters close to deep penetration threshold are chosen, see Figure 2 (b). The absence of shielding gas in the case of IR-laser welding with $d_F = 300$ μm leads to a transition from almost spatter free heat conduction welding process to process regime dominated by multiple reflections of the laser beam in the vapor capillary. As the intensity is too low for stable formation of a keyhole, the deep penetration laser welding mode collapses and initiates uncontrollable, which was observed from high-speed images. As only shielding gas application was altered between the experiments, modified heat transfer from surface oxidization is a possible reason for different process zone shaping. Beside the dependency of higher absorptivity at shorter wavelength, oxide layers significantly increase absorption of the laser radiation. The thickness and growth rate as well as the composition of the layer (CuO, Cu₂O) are found to be decisive for influencing absorptivity and thus energy coupling. [13] Without the use of a shielding gas, the copper oxidizes caused by oxygen in the ambient air. This induces higher absorptivity of sample material, shifting the process to deep penetration threshold.

3.2. Process regimes during laser welding

The transition from heat conduction to deep penetration welding using large beam diameter with green laser wavelength is shown in Figure 4. As main influencing parameters for deep penetration threshold of a material are laser power, beam diameter and laser wavelength, deep penetration process requires higher laser power in case of $d_F = 720$ μm in comparison to $d_F = 200$ μm .

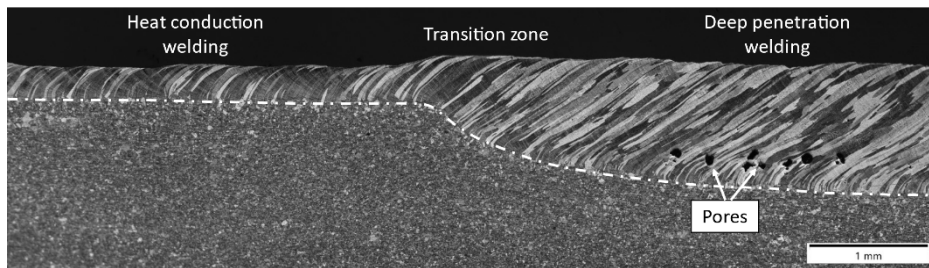


Figure 4: Longitudinal section of weld seam in Cu-ETP, transition from heat conduction (left) to deep penetration (right) welding regime; operating parameters: Cu-ETP, $t = 3$ mm, $d_F = 750$ μm , $P = 3$ kW, $v = 3$ m/min, $\lambda = 515$ nm

As can be seen, the weld seam depth increases by a factor of 3 as the process changes from heat conduction to deep penetration welding mode. Furthermore, weld seam width rises suddenly, see Figure 2 (b). Significant change in energy coupling leads to a change in temperature field as more molten volume arises. The changed cooling conditions of molten material can be observed in changing grain growth direction. Flatter angle in relation to feed rate indicates a slower cooling of the weld seam in deep penetration mode for equal processing speed. Pores are found in the lower part of the weld seam in deep penetration mode. This can result from keyhole collapses, analyzed in [14]. In addition, Alter et al. showed that there is a relation between the amount of residual oxygen content in the raw copper material and the formation of pores [15].

3.3. Deep penetration threshold and influence of larger spot diameter

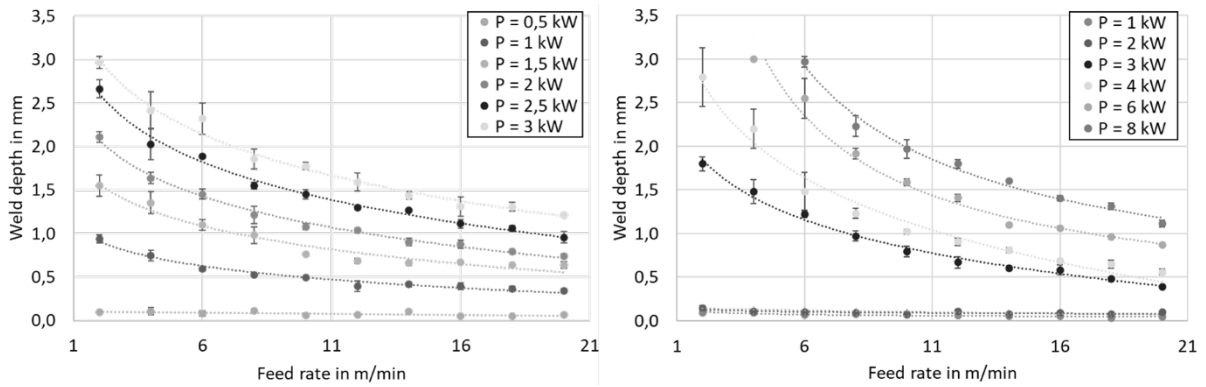


Fig. 5: Weld seam depth versus feed rate for Cu-ETP welded by different laser power ($d_F = 200 \mu\text{m}$; $\lambda = 515$ nm (left), $\lambda = 1030$ nm (right))

The resulting weld seam depths of the sample groups welded with $d_f = 200 \mu\text{m}$ are shown in Figure 5. Comparing the results for both wavelengths reveals that higher laser power is necessary in case of $\lambda = 1030 \text{ nm}$ to achieve the same weld depth in the copper sample. Higher maximum output power of IR laser system allows a through welding of 3 mm thick sample with lower energy per unit length, reducing heat input into the workpiece. A decreasing trend towards higher feed rates is observed for deep penetration welds in the range of $\geq 0,3 \text{ mm}$. This might be ascribed to as the feed rate increases, the cavity gets smaller in depth and reflection losses increase in amount while thermal conductivity losses decrease. Furthermore, an inclination of the capillary front wall accompanies. As a result, the penetration depth decreases rapidly with the feed rate as seen in Figure 5. Weld seam depths $< 0,2 \text{ mm}$ are found to be heat conduction welding seams, which do not show dependency on the feed rate. As this regime is defined by single material interaction of the laser beam (see [16]), this behaviour can be expected. Experimental investigation of deep penetration threshold is depicted in Figure 6. Therefore weld seam depth is plotted versus laser power per focal diameter for feed rate $v = 10 \text{ m/min}$. Deep penetration threshold is indicated via solid horizontal line. Framed data points show deep penetration welding results, investigated via presence of a keyhole in high-speed images.

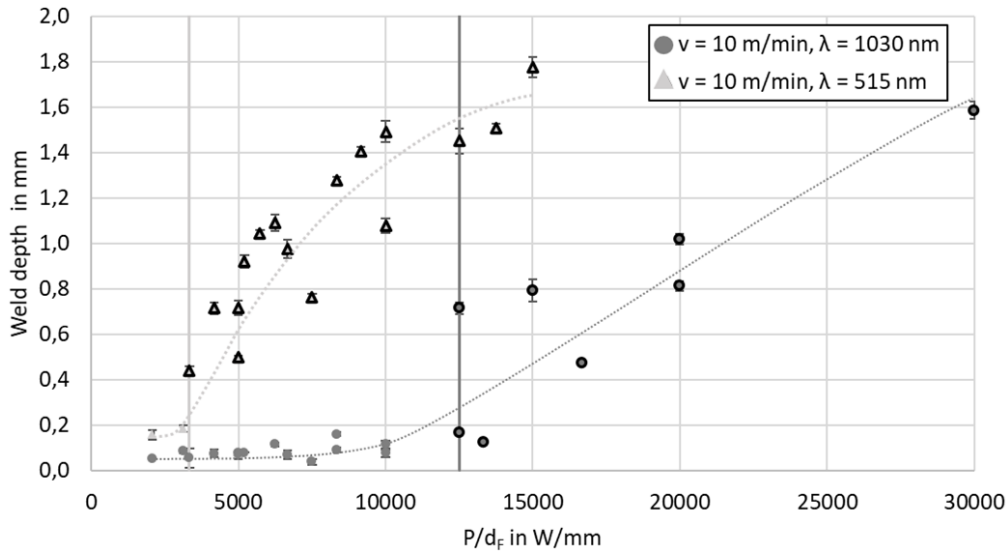


Fig. 6: Experimental investigation of deep penetration threshold: weld depth versus laser power per spot diameter for different laser wavelengths, $d_f = 200 - 480 \mu\text{m}$, $v = 10 \text{ m/min}$; data indication: no frame = heat conduction welding, framed = deep penetration welding

As can be seen, the laser power related to spot diameter describes the transition from heat conduction to deep penetration welding process in a good manner. The instantaneous transition point is observed for green wavelength at $P_T = 3333 \text{ W/mm}$ whereas it is found at 12.500 W/mm for infrared disk laser. Thus, for the green laser radiation a reduction in deep penetration threshold by a factor of 3 compared to infrared laser radiation was found. No dependence of the deep penetration welding threshold on the feed rate was detected, which is well in accordance with literature. [17] Welded samples showed constant weld mode over whole seam length apart from maximum focal diameter $d_f = 720 \mu\text{m}$ for green laser wavelength, discussed in Figure 4. This behaviour might be ascribed to the fact that with increasing focal diameter, the energy loss in the process zone increases, so that a heat accumulation only for low welding velocities contributes to a transition in weld mode. As apparent from P / d_f -ratio, significant higher laser power is required to overcome deep penetration threshold for larger spot diameters with infrared radiation. When using green laser radiation, this process regime was reached for all spot diameters investigated with laser power $P \leq 3 \text{ kW}$ using defocusing however.

Figure 7 illustrates the deep penetration laser welding process and depicts measured characteristics from high-speed images. Resulting keyhole length and width versus parameter variation is shown in the diagrams.

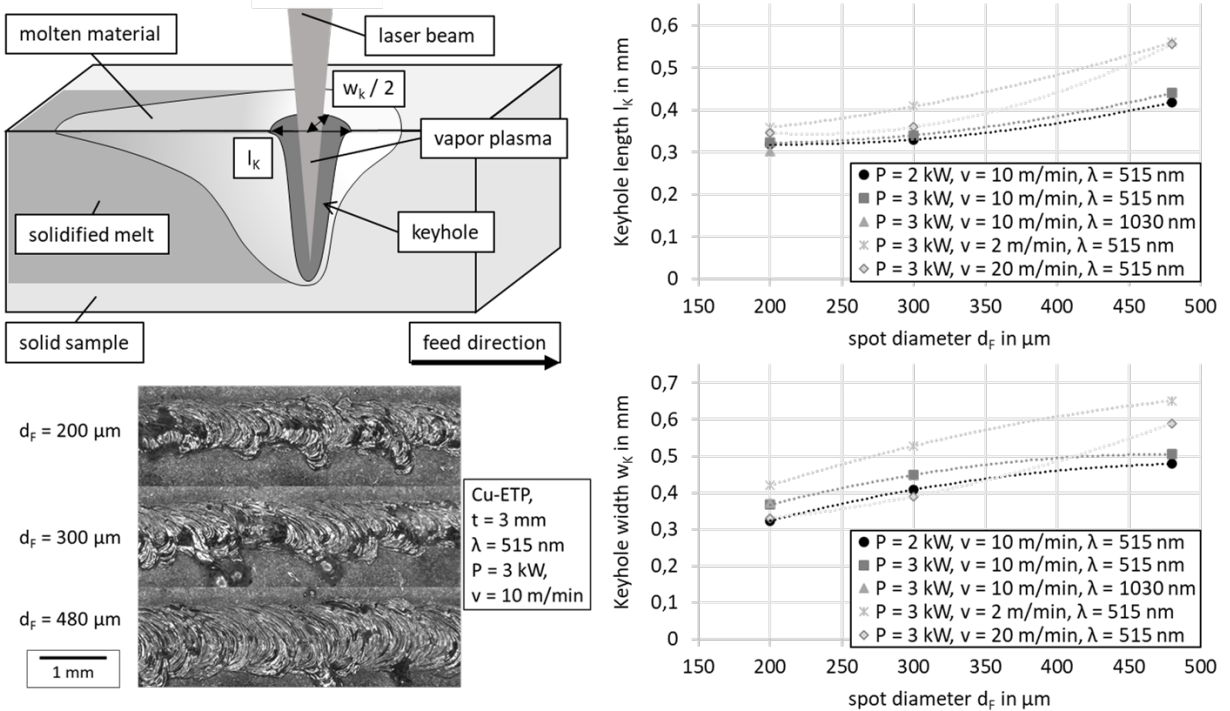


Fig. 7: High-speed investigation of welding process: analysis of keyhole dimensions for $\lambda = 515$ nm and $\lambda = 1030$ nm using beam diameters $d_f = 200 - 480 \mu\text{m}$ (right), evaluation based on manual measurements using ImageJ for $n = 20$ images per parameter set; top section of weld seams with increasing spot diameter for $\lambda = 515$ nm (bottom left, parameters see insert)

As significant higher laser power is required to initiate keyhole formation for infrared laser wavelength (see Figure 6), deep penetration welding mode in power range up to $P = 3$ kW was only observed for smallest spot diameter investigated. Increasing spot diameter d_f leads to a broadening in keyhole dimensions, leading to a broader weld seam. This can be approved by top sections of resulting weld seams, depicted in Fig. 7 bottom left for feed rate $v = 10$ m/min. In general, weld seam width is found approximately twice as wide as keyhole width, which can be attributed to high heat conductivity of copper. No significant difference for keyhole opening dimensions based on laser wavelength is observed in this work. As the feed rate increases, the keyhole opening tends to enlarge. A change in dominance of flow around the capillary versus surface tension gradient driven flow may be a reason for this finding. Low feed rate of $v = 2$ m/min also show higher feature values, caused by significant keyhole fluctuations. These result from capillary instabilities like reported in [14]. Usage of higher laser power tends to increase the keyhole opening as well, which can be explained by higher amount of energy absorbed in this area. To sum up, the laser spot diameter defines the keyhole dimensions and thus weld seam properties as enough laser power to overcome deep penetration threshold is applied.

A comparison of spattering behavior is shown in Figure 8. Therein microscopic top views and the number of spatters versus spot diameter for different laser power and wavelength used is shown. Comparing top sections of the samples one might clearly see that the surface of the weld seam becomes smoother for higher feed rates, accompanied by a narrowing of the seam width. Weld seam irregularities (spatter and melt ejections) significantly decrease for $v \geq 6$ m/min at $d_f = 200 \mu\text{m}$ with infrared wavelength, whereas a number of imperfections is still found for high feed rates with green laser radiation.

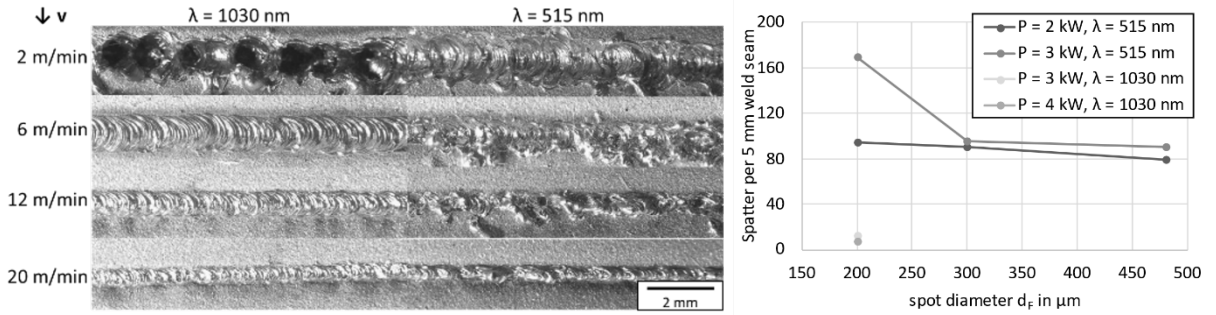


Fig. 8: Top section of weld seams with increasing feed rate from $v = 2 - 20$ m/min, $d_F = 200$ μm , $P = 3$ kW for different laser wavelength (left); spatter count per weld seam length versus spot diameter, wavelength and laser power, $v = 10$ m/min (right)

From the determined spatter count from high-speed images it becomes clear, that the number of ejections per 5 mm weld seam length significantly decreases, if a larger spot diameter is applied at $\lambda = 515$ nm. This behavior is attributed to a formed melt ring around the keyhole, able to compensate occurring keyhole fluctuations. Another possible reason is suspected in altered melt flow direction due to this enlarged melt ring [18]. The total number of observed defects scales with the laser power, as higher laser power leads to a bigger molten volume in the copper sample. The number of spatters is found significantly lower for infrared laser wavelength, also taking into account equal weld seam depth and flow conditions at $v = 10$ m/min, which is exemplary achieved at $P = 3$ kW for $\lambda = 515$ nm and $P = 6$ kW for $\lambda = 1030$ nm, compare Figure 5.

Consequently, higher absorptivity of green laser wavelength leads to an increased spatter amount even at elevated feed rates up to 20 m/min. Due to induction of higher recoil pressure at first interaction of copper sample and laser beam a continuously stronger spatter generation is observed for green laser radiation. An enlargement of the spot diameter allows to better control the spattering behavior and thus the advantages of visible wavelength to be utilized for higher weld seam quality in terms of depth and weld seam imperfections.

4. Summary

Laser beam welding of copper material with high power beam sources in the infrared and green laser wavelength was investigated within this work. Since a visible radiation shows significant higher absorption for copper, different interaction regimes and the interaction of green wavelength with the copper vapor were taken into account. It is shown, that significant higher interaction with plasma plume leads to weld seam irregularities, requiring supply of shielding gas to efficiently weld copper with green wavelength. The deep penetration welding threshold for copper material was found to be described by laser power per focal diameter in a good manner. A reduction in deep penetration threshold by a factor of 3 compared to infrared laser radiation is observed with green, resulting in a limitation of infrared wavelength to high brilliant beam sources in order to preserve stable deep penetration welding process. However, it is observed, that spattering behavior tends to be different in terms of quantitative amount of melt ejection measured. This could be explained by higher recoil pressure induced by first beam material interaction according to higher absorptivity of copper for green wavelength. It is shown that a larger beam diameter and a Gaussian intensity distribution attained by defocusing significantly reduces this spatter formation. In sum this findings lead to a better control of the joining process of copper and thus to an enhancement in weld seam quality with visible wavelength. To further optimize laser processing of copper and deeper analyze interaction of the green laser radiation with the vapor plume discussed above, a closer look on this phenomenon will be taken in further investigations via in-situ measurements of plume characteristics in deep penetration welding mode.

Acknowledgements

The authors gratefully thank the German Ministry of Economics and Energy for funding part of this work in the research project "GreenPLs: Laserbearbeitungseinheit für hochreflektive Werkstoffe" (Grant No KK5004303LP0) as part of the Central Innovation Programme for SMEs.

References

- [1] A. Heider, "Erweitern der Prozessgrenzen beim Laserstrahlschweißen von Kupfer mit Einschweißiefen zwischen 1 mm und 10 mm," doctoral thesis.
- [2] V. Dimatteo, A. Ascari, P. Faverzani, L. Poggio, and A. Fortunato, "The effect of process parameters on the morphology, mechanical strength and electrical resistance of CW laser-welded pure copper hairpins," *Journal of Manufacturing Processes*, vol. 62, pp. 450–457, 2021, doi: 10.1016/j.jmapro.2020.12.018.
- [3] S. Engler, R. Ramsayer, and R. Poprawe, "Process Studies on Laser Welding of Copper with Brilliant Green and Infrared Lasers," *Physics Procedia*, vol. 12, pp. 339–346, 2011, doi: 10.1016/j.phpro.2011.03.142.
- [4] A. Blom, P. Dunias, P. van Engen, W. Hoving, and J. de Kramer, "Process spread reduction of laser microspot welding of thin copper parts using real-time control," in 2003, pp. 493–507.
- [5] S. Amorosi, "Laser micro-spot welding of copper by real-time process monitoring: doctoral thesis," EPFL 3023, 2005.
- [6] M. Haubold, A. Ganser, T. Eder, and M. F. Zäh, "Laser welding of copper using a high power disc laser at green wavelength," *Procedia CIRP*, vol. 74, pp. 446–449, 2018, doi: 10.1016/j.procir.2018.08.161.
- [7] A. Heider, R. Weber, D. Herrmann, P. Herzog, and T. Graf, "Power modulation to stabilize laser welding of copper," *Journal of Laser Applications*, vol. 27, no. 2, p. 22003, 2015, doi: 10.2351/1.4906127.
- [8] Eva-Maria Dold et al., "Copper welding applications with a 2 kW cw laser in the green wavelength regime," in *High-Power Laser Materials Processing: Applications, Diagnostics, and Systems IX*.
- [9] *DIN EN 13601:2013-09, Kupfer und Kupferlegierungen - Stangen und Drähte aus Kupfer für die allgemeine Anwendung in der Elektrotechnik; Deutsche Fassung EN_13601:2013*, Berlin.
- [10] M. Hummel, M. Külkens, C. Schöler, W. Schulz, and A. Gillner, "In situ X-ray tomography investigations on laser welding of copper with 515 and 1030 nm laser beam sources," *Journal of Manufacturing Processes*, vol. 67, pp. 170–176, 2021, doi: 10.1016/j.jmapro.2021.04.063.
- [11] X. Zhang, M. Miyagi, and S. Okamoto, "Fundamental study on welding properties of 515nm green laser," in *International Congress on Applications of Lasers & Electro-Optics*, San Diego, CA, USA, Oct. 2014, pp. 458–462.
- [12] M. Hummel, C. Schöler, A. Häusler, A. Gillner, and R. Poprawe, "New approaches on laser micro welding of copper by using a laser beam source with a wavelength of 450 nm," *Journal of Advanced Joining Processes*, vol. 1, p. 100012, 2020, doi: 10.1016/j.jajp.2020.100012.
- [13] V. Mann, F. Hugger, S. Roth, and M. Schmidt, "Influence of Temperature and Wavelength on Optical Behavior of Copper Alloys," *AMM*, vol. 655, pp. 89–94, 2014, doi: 10.4028/www.scientific.net/AMM.655.89.
- [14] A. Heider, J. Sollinger, F. Abt, M. Boley, R. Weber, and T. Graf, "High-Speed X-Ray Analysis of Spatter Formation in Laser Welding of Copper," *Physics Procedia*, vol. 41, pp. 112–118, 2013, doi: 10.1016/j.phpro.2013.03.058.
- [15] L. Alter, A. Heider, and J. P. Bergmann, "Influence of hydrogen, oxygen, nitrogen, and water vapor on the formation of pores at welding of copper using laser light at 515 nm wavelength," *Journal of Laser Applications*, vol. 32, no. 2, 2020, doi: 10.2351/7.0000063.
- [16] R. Fabbro, M. Dal, P. Peyre, F. Coste, M. Schneider, and V. Gunenthiram, "Analysis and possible estimation of keyhole depths evolution, using laser operating parameters and material properties," *Journal of Laser Applications*, vol. 30, no. 3, p. 32410, 2018, doi: 10.2351/1.5040624.
- [17] S. M. Engler, "Laserstrahlschweißen von Kupferwerkstoffen mit brillanten Strahlquellen im infraroten und grünen Wellenlängenbereich," Dissertation, Aachen, Techn. Hochsch, Aachen, 2015.
- [18] M. Miyagi and X. Zhang, "Investigation of laser welding phenomena of pure copper by x-ray observation system," *Journal of Laser Applications*, vol. 27, no. 4, p. 42005, 2015, doi: 10.2351/1.4927609.